MedChemComm

RSC Publishing

CONCISE ARTICLE

View Article Online
View Journal

Single-walled carbon nanotubes as anisotropic relaxation probes for magnetic resonance imaging†

Cite this: DOI: 10.1039/c3md20235f

Arisbel Cerpa,[a] Mariana Köber,[b] Daniel Calle,[c] Viviana Negri,[d] Jose María Gavira,[e] Antonio Hernanz,[e] Fernando Briones,[b] Sebastián Cerdán[c] and Paloma Ballesteros*[d]

Received 9th August 2012
Accepted 4th February 2013

DOI: 10.1039/c3md20235f

www.rsc.org/medchemcomm

We report on the preparation and characterization of magnetically oriented single-walled carbon nanotube arrangements as novel nanoprobes to enhance anisotropically water relaxation as detected by magnetic resonance imaging methods. SWCNT suspensions immobilized in agarose gels showed evident magnetic anisotropy with significantly longer T_2 in the parallel than in the perpendicular orientations.

Magnetic Resonance Imaging (MRI) has become one of the most powerful tools in modern medical diagnosis because of its non-invasive character, high inherent spatial resolution and the possibility to enhance locally and specifically image intensity using appropriate paramagnetic or superparamagnetic contrast agents (CAs). Most of the MRI CAs currently available are chelates of paramagnetic metals of the rare earth series or superparamagnetic iron oxide nanoparticles, the Gd(III) chelates being the most widely used.[1] In all these cases, the induced relaxation of the water molecules surrounding the probe is isotropic precluding the encoding of directionality in many fundamental biological processes already detectable by molecular imaging.[2,3]

On these grounds, it would entail considerable relevance to develop CAs in which the predominant molecular orientation of the probe with respect to the external magnetic field can be inferred from the non-invasive MRI measurement. We have previously shown that SWCNT suspensions are excellent candidates for this purpose, since they orient parallel to the external magnetic field and induce faster translational diffusion of water molecules moving along their longitudinal axis.[4] Here we extend this approach to describe the preparation, physicochemical and toxicological characterization of magnetically and chemically active SWCNTs by inducing anisotropic water relaxation detectable by MRI.

In order to obtain sufficiently soluble and functionalized SWCNT preparations,[5] suitable for diagnostic or therapeutic applications,[6] both nanotube length and chemical inertness of the surface need to be optimized. In particular, CNT preparations are known to contain significant amounts of paramagnetic metals[7] and amorphous carbon derived from their process of synthesis. These crude preparations must be purified to remove unwanted paramagnetic impurities and amorphous carbon, while preserving the highly organized SWCNT structure. Four major methods have been proposed for this purpose: acid oxidation, gas oxidation, filtration, and chromatography.[8,9] It is widely accepted that the content of nanotubes can be increased selectively by oxidation, since the etching rate of amorphous carbons is faster than that of nanotubes. Purification through acid treatment often provides a complementary method to oxidation. Acid treatment causes the ends and sidewalls of the oxidized nanotubes to become functionalized with carboxylic groups useful for further processing. However, the acid management may eventually cause extensive disruption of the CNT nanotubular structure[10] and defects in sidewalls,[11–13] hampering further utilization. Optimization of this process then becomes mandatory to preserve adequate nanotubular structure and properties and minimize its deleterious effects.

In this work, we report on an optimized nitric acid oxidation protocol[14] using as starting materials commercial single-walled carbon nanotubes (Aldrich, 40–60%, prepared by chemical vapour deposition, CVD), having initially diameters of 2–10 nm and lengths of 1–5 μm contaminated with residual 17% Ni and 4% Y. We investigated systematically 24 and 48 h oxidation times. A suspension of SWCNTs (200 mg) in HNO_3 (25 ml) was heated under reflux. The reaction mixture was cooled and diluted with deionized water (100 ml). The resulting suspension

[a]Department of Electromechanics and Materials, Universidad Europea de Madrid, C/Tajo, s/n. Villaviciosa de Odón, Madrid-28670, Spain. E-mail: arisbel.cerpa@uem.es; Fax: +34 916168265; Tel: +34 912115658

[b]IMM, Institute of Microelectronics of Madrid, CNM, CSIC, Madrid-28760, Spain. E-mail: mariana.koeber@imm.cnm.csic.es; Fax: +34 948060701; Tel: +34 918060700

[c]Institute of Biomedical Research "Alberto Sols", CSIC, Madrid-28029, Spain. E-mail: scerdan@iib.uam.es; Fax: +34 915854587; Tel: +34 915854444

[d]Laboratory of Organic Synthesis and MRI, Faculty of Sciences, UNED, Associated Unit CSIC, Madrid-28040, Spain. E-mail: pballesteros@ccia.uned.es; Fax: +34 913986697; Tel: +34 913987117

[e]Department of Experimental Physico-Chemical Sciences, Faculty of Sciences, UNED, Madrid-28040, Spain. E-mail: ahernanz@ccia.uned.es; Fax: +34 913986697; Tel: +34 913987377

† Electronic supplementary information (ESI) available. See DOI: 10.1039/c3md20235f

was centrifuged at 3000 rpm for 10 min and the precipitate was resuspended in deionized water and placed in a dialysis membrane to be washed until the pH reaches *ca.* 5.5. The dialyzed suspension was centrifuged to isolate the NTs which were dried in a desiccator. TXRF analysis of the oxidized CNTs showed residual paramagnetic metals of 3.2% Ni and 0.64% Y or 5.9% Ni and 1.17% Y after 24 or 48 hours of oxidation, respectively (see ESI†). This behaviour has been previously reported.[17] Increasing the oxidation times further to 72 and 96 h was not investigated since extensive decomposition was detected. TEM analysis revealed the classical carbon nanotubular structure and SWCNT bundles, as well as some amorphous carbon residues and metallic nanoparticles from the catalyst (Fig. 1A). Individual nanotubes can also be observed using Atomic Force Microscopy (AFM, Fig. 1B), allowing the determination of nanotube shortening along the nitric acid oxidation process (Fig. 1C). While untreated SWCNTs showed lengths from 1 to 5 μm, nanotube preparations oxidized for 24 h showed a length distribution between 200 and 700 nm, with the most numerous components sized *ca.* 300 nm (Fig. 1D).

Raman spectroscopy was implemented to determine the structural changes that oxidation could induce in the nanotube preparations. Raman spectra (Fig. 2) showed the typical features of SWCNTs: tangential modes (or G bands), radial breathing modes (RBMs) and a D band. For the untreated SWCNTs the split G band (1578 and 1585 cm^{-1}) and the G′ band (2500–2800 cm^{-1}) depicted high intensity, a sign of well-organized graphene. An additional peak at 1315–1325 cm^{-1} (D band)[15] is present with significantly lower intensity, roughly proportional to the amount of amorphous carbon in the sample. This band has also been previously assigned to disordered or sp^3-hybridized carbons in the hexagonal framework of the nanotube walls.[15] In addition, two bands corresponding to the radial breathing mode (RBM, around 145 and 160 cm^{-1}) are further

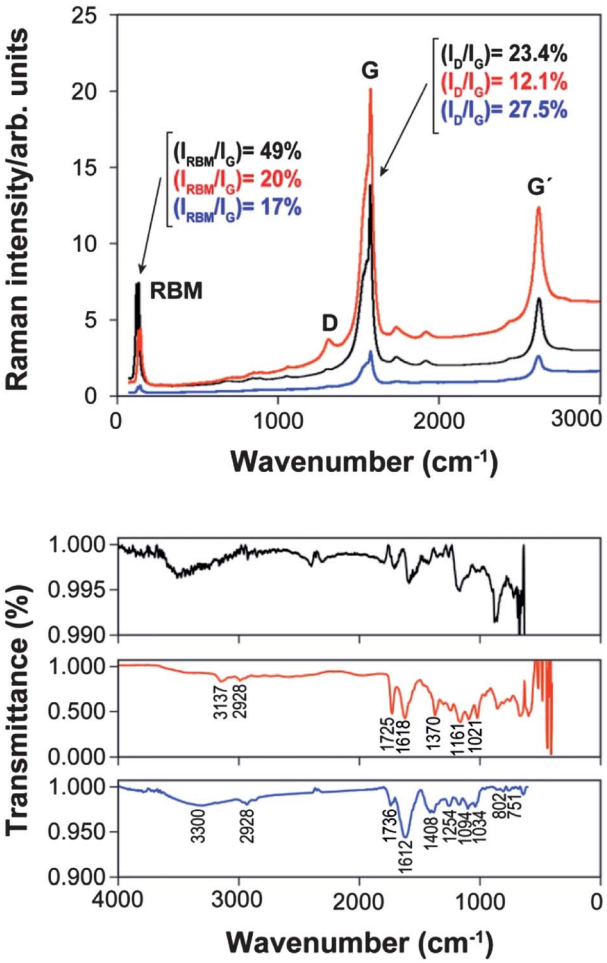

Fig. 2 Raman (upper panel) and IR (lower panels) spectra of untreated commercial nanotubes (black) and nanotubes resulting from 24 h (red) and 48 h (blue) oxidation times.

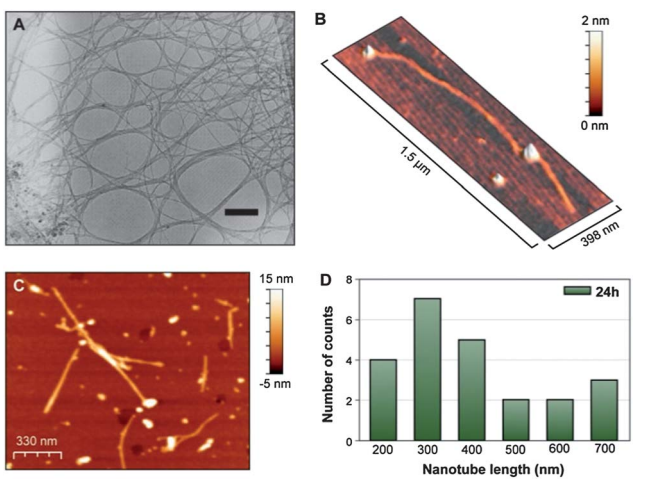

Fig. 1 (A) TEM image of SWCNTs after 48 hours of nitric oxidation (scale bar represents 200 nm) shows high density of nanofilament entanglements, (B) typical AFM image of SWCNTs before oxidation, (C) typical AFM image of SWCNTs after oxidation for 24 hours, and (D) histogram of SWCNT lengths from SWCNTs oxidized for 24 h as obtained from AFM measurements. Note that the nanotube length is conveniently shortened under these conditions.

observed. After 24 h of oxidation, the intensities of the G and G′ bands remained high, revealing the maintenance of an adequately organized graphene structure.[16] Due to the heterogeneity of the SWCNT preparations and the microscopic Raman determinations used, longer oxidation times could not be directly related with the intensity of the D and G bands as previously stated.[17] However, the nanotubular structure is clearly established not only by the G bands but also by the radial breathing bands (RBM) at around 145 and 160 cm^{-1}. Untreated SWCNTs present 49% of RBM/G ratio, while after 24 h and 48 h oxidation times the RBM/G ratio decreases to 20% and 17% respectively (Fig. 2, upper panel). These features suggest that 24 h can be considered as an optimum compromised oxidation time which allows SWCNTs with both carboxylic groups and nanotubular structure suitable in the study of magnetic resonance anisotropy.

The IR spectra of the oxidized preparations confirmed the presence of carboxylic groups through the presence of characteristic C=O and O–H stretching bands at *ca.* 1700 and 3200 cm^{-1}, respectively (Fig. 2, lower panel).

We investigated then the magnetic relaxation properties of water in the different preparations of untreated and oxidized

SWCNTs. We previously reported that SWCNT preparations depict a superparamagnetic character, mainly reflecting the presence of residual metal contaminants.[4] Here, we measured the T_1 and T_2 relaxation times (Bruker Minispec, 1.5 Tesla, 22 °C) of water (3196 ± 21 and 2667 ± 3.9 ms) and homogeneously suspended oxidized SWCNT preparations (1 mg ml^{-1}) in an aqueous solution of 2% sodium dodecylbenzene sulphonate (SBDS). T_1 and T_2 values in SWCNT suspensions (0, 24, 48 h) were (1301 ± 8, 2049 ± 5, 1425 ± 5 ms) and (63 ± 0.0, 292 ± 0.1, 139 ± 0.1 ms), respectively. These results agree with previous reports indicating a stronger effect of unoxidized SWCNTs in T_2 than in T_1, consistent with their superparamagnetic character.[18] Notably, increases in the oxidation time lead to significant increases in the T_1 and T_2 relaxation times of water of the oxidized SWCNTs as compared to the untreated preparations, reflecting most probably the progressive removal of paramagnetic contaminants along the oxidation process. Increases in the relaxation times observed at 48 h were smaller than at 24 h, a circumstance probably related to the damaged nanotubular structure characterized previously by Raman spectroscopy.

To explore the directional dependence of the magnetic relaxation properties of SWCNTs, untreated SWCNTs (0.5 mg) were suspended in 200 μl fetal calf serum (14 kW, 1 h, Soniprep 150 MSE, London, UK), and thoroughly mixed with an equal amount of hot, melted, agarose (60 °C, 0.5%, A6013 Sigma-Aldrich, St. Louis, MO, USA). The melted SWCNT agarose suspension was then layered in an Eppendorf tube, on top of a bed of previously solidified agarose (to minimize the amount of SWCNTs required), and the whole arrangement was allowed to cool down to room temperature overnight, while being placed in the isocenter of a 7 Tesla horizontal magnet (Bruker Biospin, Ettlingen, DE).

This protocol resulted in solid agarose gels containing in the upper phase the immobilized SWCNT suspension, oriented in the direction of the applied static magnetic field B_0, and in the lower phase the solid agarose bed only. The Eppendorf tube was then accommodated in a homemade goniometer (Fig. 3A) which allowed the manual rotation of the tube with respect to the external magnetic field. We then obtained T_2 maps (CPMG sequence, TR: 5000 ms, TE: 12–600 ms) with the nanotube preparation oriented in two orthogonal directions, either parallel or perpendicular to the magnetic field (Fig. 3B). Notably, T_2 values were found to be significantly longer in the parallel than in the perpendicular orientations (Fig. 3C). We did not observe any anisotropy effects in relaxation when plain agarose suspensions were investigated, indicating that the anisotropic effects observed arise from the SWCNTs. This may probably reflect the larger magnetic susceptibility and local magnetic field of the nanotubes along their longitudinal direction, inducing a larger increase in the T_2 of water molecules located in the extremes of the nanotube than in those placed at the sidewalls. Interestingly, the observed rotational variation of T_2 is larger in magnitude than the one previously detected for the Apparent Diffusion Coefficient (ADC) of water in these preparations,[4] suggesting that directional relaxation measurements may provide a more sensitive method than

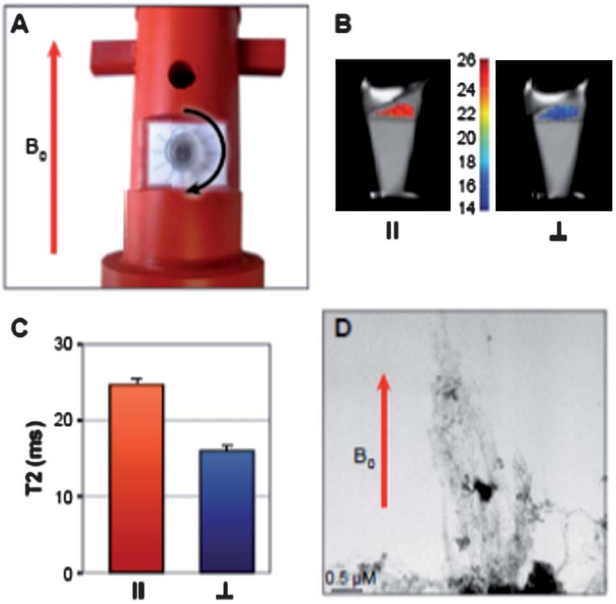

Fig. 3 (A) Homemade PVC goniometer for MRI measurements of the angular dependence of water relaxation in Eppendorf tubes containing solid, magnetically oriented SWCNT gels in the upper phase and solid agarose in the lower phase. (B) T_2 maps of untreated nanotube suspensions oriented parallel or perpendicular to B_0. Note the longer T_2 in the parallel orientation. (C) Bar graph showing pixel values of T_2 in the parallel (red) and perpendicular (blue) orientations. (D) TEM image (200 kV) illustrating the predominant alignment of nanotube bundles along the static magnetic field.

translational diffusion to infer molecular orientation. It should be mentioned here that anisotropic relaxation effects with a similar magnitude to that reported herein for SWCNTs have been previously reported for oriented collagen fiber preparations, both *in vivo* and *in vitro*.[19,20] This suggests that the SWCNT preparations reported here may become efficient probes for anisotropy even *in vivo*, reaching similar values to those previously observed in endogenously available collagen fibers. Moreover, the detected changes in T_2 between the two orthogonal orientations of SWCNT suspensions may be further augmented either by increasing the concentration of SWCNTs in the gel, increasing their intrinsic paramagnetic properties introducing lanthanide ions[21] and chelates, or by reducing the nanotube entanglements that prevent the completely parallel alignment of individual SWCNT structures along the magnetic field. To investigate this aspect, we observed the orientation of the nanotube preparations under these conditions, using TEM measurements. Fig. 3D shows a representative TEM image from magnetically oriented SWCNTs, showing a predominant orientation of the nanotube bundles parallel to the magnetic field, but also the presence of residual, insufficiently oriented, entangled bundles precluding a complete and homogeneous alignment of all nanotubular structures along the B_0 field.

Finally, we investigated *in vitro* the toxicity of the SWCNT preparations (1–1000 μg ml^{-1}) oxidized for 24 h, as prepared in this study, using the MTT and LDH release methods[22,23] and cultures of C6 cells (see ESI†). Briefly, the MTT assay showed increased formazan production in this range, an effect

previously reported to be due to a direct chemical reaction of the SWCNTs with MTT, rather than to a reduced cellular viability.[23] In fact, we observed no significant increase in LDH release in this concentration range suggesting no appreciable cytotoxicity, as described earlier.[23]

In conclusion, in this Communication we presented a systematic study on the preparation, physicochemical and toxicological properties of SWCNTs oxidized for increasing times, as directional relaxivity probes for MRI. Shortening graphene structure and T_2 enhancement properties are shown to be better after 24 h than after 48 h of oxidation. SWCNT suspensions prepared in melted agarose gels can be conveniently oriented in an external magnetic field exhibiting, after solidification by cooling, significant anisotropic MRI relaxivity properties in T_2 with longer values in the parallel than in the perpendicular orientations.

We thank grants CTQ2010-20960-C02-01, P2010/BMD-2349, and SAF2011/23622. The present work is a result of the collaboration UNED–CSIC Associated Unit of Molecular Imaging by Magnetic Resonance. M. K. and V. N. acknowledge financial support through I3P and JAE fellowships, respectively.

Notes and references

1 É. Tóth, L. Helm and A. E. Merbach, in *The Chemistry of Contrast Agents in Medical Magnetic Resonance Imaging*, ed. A. E. Merbach and É. Tóth, John Wiley & Sons, Ltd., Chichester, 2001, ch. 2.
2 S. Aime, D. D. Castelli, S. G. Crich, E. Gianolio and E. Terreno, *Acc. Chem. Res.*, 2009, **42**, 822–831.
3 D. Pan, S. D. Caruthers, J. Chen, P. M. Winter, A. SenPan, A. H. Schmieder, S. A. Wickline and G. M. Lanza, *Future Med. Chem.*, 2010, **2**, 471–490.
4 V. Negri, A. Cerpa, P. López-Larrubia, L. Nieto, S. Cerdán and P. Ballesteros, *Angew. Chem., Int. Ed.*, 2010, **49**, 1813–1815.
5 B. Sitharaman, K. B. Kisell, K. B. Hartman, L. A. Tran, A. Baikalov, I. Rusakova, Y. Sun, H. A. Khant, S. J. Ludtke, W. Chiu, S. Laus, E. Tóth, A. E. Merbach and L. J. Wilson, *Chem. Commun.*, 2005, 3915–3917.
6 C. Richard, B. T. Doan, J. C. Beloeil, M. Bessodes, E. Tóth and D. Scherman, *Nano Lett.*, 2008, **8**, 232–236.
7 I. W. Chiang, B. E. Brinson, R. E. Smalley, J. L. Margrave and R. H. Hauge, *J. Phys. Chem. B*, 2001, **105**, 1157–1161.
8 H. Peng-Xiang, L. Chang and C. Hui-Ming, *Carbon*, 2008, **46**, 2003–2025.
9 A. G. Rinzler, J. Liu, H. Dai, P. Nikolaev, C. B. Huffman, F. J. Rodriguez-Macias, P. J. Boul, A. H. Lu, D. Heymann, D. T. Colbert, R. S. Lee, J. E. Fischer, A. M. Rao, P. C. Eklund and R. E. Smalley, *Appl. Phys. A: Solid Surf.*, 1998, **67**, 29–37.
10 M. Monthioux, B. W. Smith, B. Burteaux, A. Claye, J. E. Fisher and D. E. Luzzi, *Carbon*, 2001, **39**, 1251–1272.
11 V. Ivanov, A. Fonseca, J. B. Nagy, A. Lucas, P. Lambin, D. Bernaerts and X. B. Zhang, *Carbon*, 1995, **33**, 1727–1738.
12 E. Borowiak-Palen, T. Pichler, X. Liu, M. Knupfer, A. Graff, O. Jost, W. Pompe, R. J. Kalenczuk and J. Fink, *Chem. Phys. Lett.*, 2002, **363**, 567–572.
13 H. Hu, P. Bhowmik, B. Zhao, M. A. Hamon, M. E. Itkis and R. C. Haddon, *Chem. Phys. Lett.*, 2001, **345**, 25–28.
14 A. B. Bourlinos, V. Georgakilas, V. Tzitzios, N. Boukos, R. Herrera and E. P. Giannelis, *Small*, 2006, **2**, 1188–1191.
15 M. S. Dresselhaus, G. Dresselhaus, R. Saito and A. Jorio, *Phys. Rep.*, 2005, **409**, 47–99.
16 M. S. Dresselhaus, A. Jorio, M. Hofmann, G. Dresselhaus and R. Saito, *Nano Lett.*, 2010, **10**, 751–758.
17 B. Ballesteros, G. Tobias, L. Shao, E. Pellicer, J. Nogués, E. Mendoza and M. L. H. Green, *Small*, 2008, **4**, 1501–1506.
18 J. S. Ananta, M. L. Matson, A. M. Tang, T. Mandal, S. Lin, K. Wong, S. T. Wong and L. J. Wilson, *J. Phys. Chem. C*, 2009, **113**, 19369–19372.
19 M. Bydder, A. Rahal, G. D. Fullerton and G. M. Bydder, *J. Magn. Reson. Imaging*, 2007, **25**, 290–300.
20 S. J. Erickson, R. W. Prost and M. E. Timmins, *Radiology*, 1993, **188**, 23–25.
21 B. Sitharaman, K. R. Kissell, K. B. Hartman, L. A. Tran, A. Baikalov, I. Rusakova, Y. Sun, H. A. Khant, S. J. Ludtke, W. Chiu, S. Laus, E. Toth, L. Helm, A. E. Merbach and L. J. Wilson, *Chem. Commun.*, 2005, 915–917.
22 T. Mosmann, *J. Immunol. Methods*, 1983, **65**, 55–63.
23 J. M. Wörle-Knirsch, K. Pulskamp and H. F. Krug, *Nano Lett.*, 2006, **6**, 1261–1268.

